

Modeling the Resilience of Power Distribution Systems Against Extreme Winds by Considering Falling Trees

Guangyang Hou

*School of Civil Engineering and Environmental Science
University of Oklahoma
Norman, OK, USA
guangyang.hou@ou.edu*

Kanthasamy K. Muraleetharan

*School of Civil Engineering and Environmental Science
University of Oklahoma
Norman, OK, USA
muralee@ou.edu*

Abstract—Overhead electrical power distribution systems (PDS) are very susceptible to extreme wind events such as hurricanes and typhoons. Power outages can cause catastrophic consequences, including economic loss, loss of other critical services, and disruption of daily life. Therefore, it is very important to model the resilience of PDS against extreme winds to support disaster planning. Although falling trees are one of the main causes of PDS failures, the tree-failure risk was rarely considered in the performance assessment of PDS in the literature. In this study, a probabilistic simulation framework is proposed to model the resilience of PDS against extreme winds, in which the tree-failure risk can be realistically considered. The framework is demonstrated with a power distribution network in Oklahoma. Results show that the system resilience can reduce by 24% if tree failures are considered. In addition, crown thinning can effectively enhance the system resilience but will become less effective when the wind speed is very low or high.

Keywords—resilience, enhancement, power distribution system, fragility, falling trees, crown thinning

I. INTRODUCTION

Overhead electrical power distribution systems (PDS) are very susceptible to extreme wind events such as hurricanes and typhoons. Extreme wind-caused disruption of PDS is responsible for most of the power outages that occur in the United States. Power outages can cause catastrophic consequences, including economic loss, loss of other critical services (e.g., water, transportation, communication, and healthcare), and disruption of daily life. For example, during Hurricane Ida in 2021, up to 1.2 million customers lost their power across eight states in U.S.

Extreme wind events such as hurricanes and typhoons can cause widespread damage to power poles, lines, and trees. The falling trees or limbs can further cause extensive disruption to overhead PDS. For example, tree failures are responsible for about 55.2% of PDS failures in the Northeast U.S. [1]. Despite severe consequences caused by falling trees, very limited effort has been put into modeling tree fragility and assessing tree-induced risk to PDS components [2-4]. As a result, tree-induced risk has not been systematically considered in the resilience modeling of PDS against extreme winds.

In this study, a probabilistic simulation framework is proposed to model the resilience of PDS against extreme winds, in which the tree-failure risk can be realistically considered. In this framework, first, windthrow fragility curves are developed; second, fragility curves of PDS components under wind or tree loads are developed; third, PDS component failure is estimated based on fragility curves of trees and PDS components, and the relative location of trees and conductors; fourth, the PDS performance is evaluated with a connectivity-based method; fifth, the PDS is restored by considering uncertain component repair time and component criticality; finally, crown thinning is used to enhance the PDS resilience. The framework is demonstrated with a power distribution network in Oklahoma.

II. SIMULATION FRAMEWORK

A simulation framework for assessing the resilience of PDS subjected to extreme winds is introduced in this section. The proposed framework includes six parts: windthrow fragility modeling, PDS component fragility modeling, PDS component failure estimation, system performance evaluation, system restoration, and resilience enhancement with vegetation management. The details of each part of the framework are presented below.

A. Windthrow fragility modeling

In this study, a fragility modeling method proposed by Hou and Chen [2] is used to develop windthrow fragility curves. Allometric equations are developed based on measured data. With allometric equations, some hard to measure parameters can be predicted with an easily measured one. For the allometric equations developed in this study, parameters such as diameter at breast height (DBH), crown height, and crown diameter are expressed as functions of the tree height. A finite element tree model as shown in Fig. 1 is built to compute the internal forces of the tree structure under winds. A tapered tree stem is discretized into multiple beam elements with uniform cross-sections. The cross-section in the middle of an element is used to represent the property of this element. Static wind loads are applied to both the stem and crown. The 3-s gust wind speed is used to calculate the wind forces; the wind profile is assumed to follow the power-law form. When calculating the wind force on the tree crown, it is assumed that the crown has a triangular shape. In addition, the weight of the stem and crown are also considered in the finite element model. The tree structure is fixed at the bottom. To consider the P-Delta effects due to the tree self-weight, the second-order analysis is performed by including the geometric stiffness matrix in the total stiffness matrix..

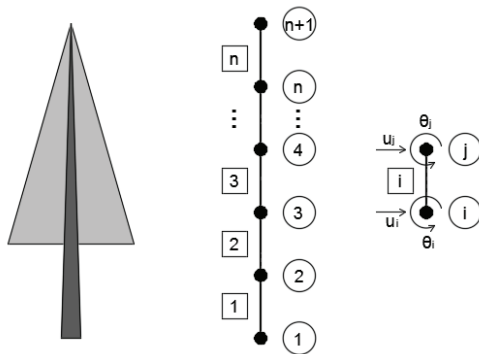


Fig. 1. Finite element model of a tree

Two common failure modes for urban trees under extreme wind conditions are identified: stem breakage and uprooting [2]. Stem breakage is defined as when the maximum compressive stress in the stem exceeds the stem modulus of rupture while uprooting refers to the situation when the critical turning moment provided by the root-soil plate anchorage is exceeded by the base turning moment produced by wind. Fragility curves of two

failure modes are developed after running 10,000 Monte Carlo simulation trials. Further details about the windthrow fragility modeling method can be found in the reference [2]

B. PDS component fragility modeling

During extreme wind events, PDS components can be damaged by either the wind directly or falling trees indirectly. In the wind scenario, common failure modes are bending failure of poles and conductor breakage. In the tree scenario, conductor breakage and short circuit are prevalent failure modes. Pole failure occurs when the maximum stress due to external loads exceeds the fiber strength of poles. Conductor breakage occurs when the breaking strength of conductors is exceeded by the maximum stress caused by external loads. A short circuit occurs when the phase conductor is close enough to the neutral conductor under the weight of falling trees. This type of short circuit only applies to a 1-phase line system. For a 3-phase line system, the short circuit is assumed to occur once a tree falls on it. This is because conductors in a 3-phase line system are in an approximately horizontal plane and a bridge between different conductors is easily formed in this case. A simulation-based approach is used to develop fragility curves of different failure modes [5]. For a given pole-wire system, the Latin Hypercube sampling method is employed to generate random samples for uncertain parameters related to demand and capacity. For each realization, a 3-span power-wire system is modeled in the finite element computer code, ANSYS, to calculate the structural response under external wind and tree loads, as shown in Fig. 2.

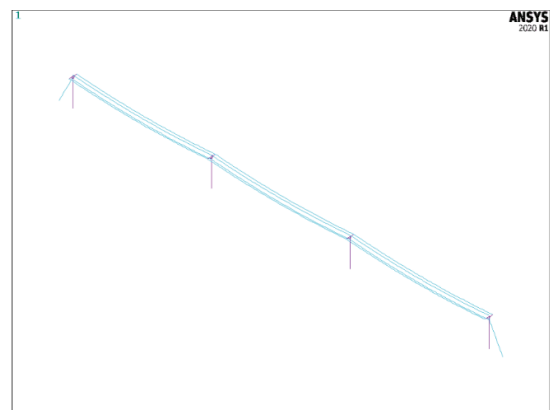


Fig. 2. Finite element model of a 3-span 3-phase power-wire system in ANSYS

Damage states of PDS components are determined by checking limit state functions of failure modes.

Failure probability for a given hazard intensity is obtained after running 3,000 Monte Carlo simulation trials, and fragility curves are developed after covering a wide range of hazard intensity.

C. PDS component failure estimation

With windthrow fragility and PDS component fragility, the probability of failure of different PDS components can be calculated. The failure probability of pole i can be computed with Eq. (1).

$$p_{f,pole,i} = p_{bd,w,i} \quad (1)$$

where $p_{bd,w,i}$ is the bending failure probability of pole i due to wind load. The failure probability of conductor j can be calculated by:

$$p_{f,conductor,j} = \max(p_{br,w,j}, p_{tree,j} p_{br,t,j} f_j, p_{tree,j} p_{st,t,j} f_j) \quad (2)$$

where $p_{br,w,j}$ is the breakage probability of conductor j due to wind load; $p_{br,t,j}$ and $p_{st,t,j}$ are the breakage and short circuit probability of conductor j due to falling trees, respectively; $p_{tree,j}$ is the damage probability of trees along conductor j , $p_{tree,j} = 1 - (1 - p_{tree,w})^n$; $p_{tree,w}$ is the failure probability of a single tree due to wind load; n is the number of hazard trees along conductor j ; f_j indicates the consequence of falling trees along conductor j , if a falling tree falls on it, $f_j = 1$, otherwise, $f_j = 0$. As shown in Fig. 3, if Eq. (3) or Eq. (4) is satisfied, a broken or uprooted tree will fall on the power line.

A broken tree falls on the power line:

$$H_b > H' = \sqrt{h'^2 + d'} \quad (3)$$

An uprooted tree falls on the power line:

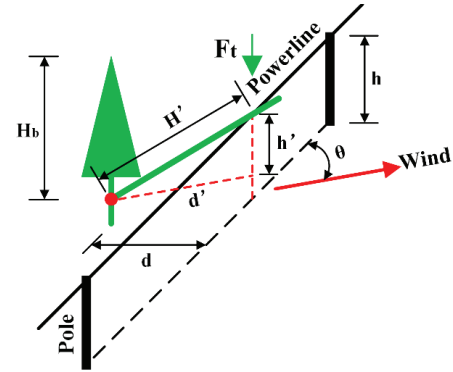
$$H > H' = \sqrt{h^2 + d'} \quad (4)$$

where h is the height of the powerline (m); $d' = d/\sin(\theta)$, d is the distance between the tree and the powerline (m); $h' = h - (H - H_b)$. Currently, the dynamic effect of falling trees is not considered for simplicity; only the static load is applied to the conductors. The load of a falling tree acting on the power line in the broken and uprooted tree scenarios can be calculated with Eqs. (5) and (6), respectively.

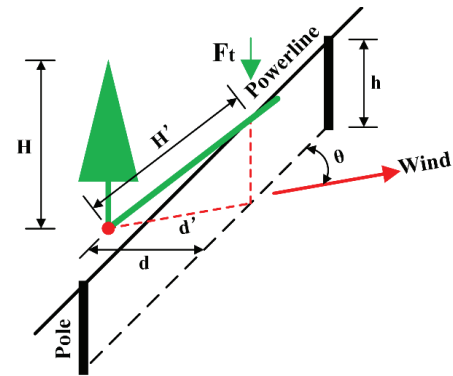
$$F_t = \frac{W_{tb}H_b}{2H'} \quad (5)$$

$$F_t = \frac{W_t H}{2H'} \quad (6)$$

where W_{tb} is the weight of the broken tree; W_t is the weight of the uprooted tree. In scenarios when there is more than 1 tree along a conductor, it is assumed that the f_j and F_t is determined by the biggest tree.



(a) Stem breakage



(b) Uprooting

Fig. 3. Schematic diagrams of falling-tree scenarios

D. System performance evaluation

A connectivity-based method, as shown in Fig. 4, is used to evaluate the performance of radial distribution systems in this study. First, a network consisting of nodes and edges is used to represent a distribution system. The nodes and edges represent the poles and conductors, respectively. All paths connecting customers and the substation are identified. Each path is a set of nodes and edges. Second, the protective devices (e.g., switches, fuses, reclosers, and circuit breakers) that affect the power flow of each path are identified. If at least one of these devices is open, the path is disconnected. Third, components (poles and conductors) that can trip each protective device are identified. If at least one of these components fails, the protective device is open. Finally, the connectivity of each path is determined by the state of protective devices. After the connectivity of all

paths is known, the PDS performance, namely, the ratio of customers with power, can be evaluated with Eq. (7).

$$Q(t) = \frac{N_0(t)}{N} \quad (7)$$

where $Q(t)$ is the system performance at time t ; $N_0(t)$ is the number of customers with power at time t ; N is the total number of customers.

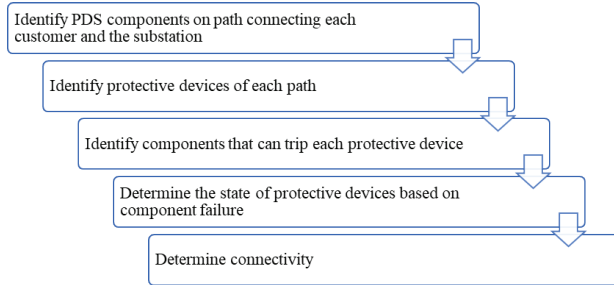


Fig. 4. Flowchart of connectivity-based method

E. System restoration

Rapid restoration of PDS after natural disasters can not only reduce the loss caused by power outages but also expedite the restoration of other infrastructures which are dependent on PDS. Three factors must be considered in the post-disaster restoration: restoration resources, restoration time, and restoration sequence. Restoration resources refer to the number of repair teams, consisting of repair crews, equipment, and material. It is assumed that a failure only requires one repair team for the restoration. To consider the uncertainty in component restoration time, the normal distribution is used to describe the restoration time of different failures. In this study, the restoration time (in hours) for a pole failure, a conductor failure, and a tree-induced short circuit has the distribution $t_{pole} \sim N(5, 2.5)$, $t_{conductor} \sim N(4, 2.0)$, and $t_{short} \sim N(1, 0.5)$, respectively [6]. To maximize the PDS resilience, restoration priority should be given to the critical components connected to the greatest number of customers. In this study, the restoration sequence is determined by the component criticality, which is measured with a critical index (CI). The critical index of a component is defined as the change in system performance (i.e., the number of customers with power) when the component is removed from the system. Component CI can be calculated with Eq. (8).

$$CI_i = 1 - Q(\delta_i = 0) \quad (8)$$

where δ_i is the state indicator of component i , if component i fails, $\delta_i = 0$ or else $\delta_i = 1$; $Q(\delta_i = 0)$ is the system performance when only component i fails but others still operate. All components are ranked based on their CI . Typically, components on the mainline and close to the substation have a relatively high CI ranking and high restoration priority. The resilience of PDS is evaluated with Eq. (9).

$$RI = \frac{\int_{t_0}^{t_0+t_c} Q(t) dt}{t_c} \quad (9)$$

where RI is the resilience index; t_0 is the time when the power network is hit by a wind event; t_c is the control time. The expected energy not supplied (EENS) is calculated with Eq. (10).

$$EENS = \sum_{i,t} P_{i,t} \quad (10)$$

where $P_{i,t}$ is the lost load of customer i at time t .

F. Resilience enhancement with vegetation management

It is not economical and environment-friendly to remove all hazardous trees that threaten PDS. A common measure to reduce the windthrow risk without affecting tree health is crown thinning. Crown thinning, as one of the vegetation management methods, involves the selective removal of stems and branches to produce an evenly spaced branch structure. Through crown thinning, the crown weight is reduced. In addition, because of the reduction in the ventilation ratio of the crown, the wind loads acting on the crown are also reduced. Therefore, crown thinning can reduce the windthrow likelihood of a tree and further reduce the tree-failure risk to PDS.

III. ILLUSTRATIVE EXAMPLE

The proposed framework is applied to a power distribution network in Oklahoma. Fig. 5 shows the layout of the power distribution network, which consists of 770 wood poles and 769 conductors. Bur oaks are the most common trees in the area where the power distribution network is located. Hazard trees, which are close to and taller than power lines, are identified with Google Earth. The height of hazard trees and the distance to power lines are recorded. Fig. 5 also shows the number of hazard trees along conductors. There are three pole classes: Class 2, 4, and 5, accounting for 30.5%, 64.9%, and 4.6% of the total number of poles, respectively. The substation is located at the northernmost part of the network. In addition, there are many protective

devices in the network such as switches, fuses, line sectionalizers, reclosers, and circuit breakers, although they are not shown in the figure. Other network data includes power line phase, power line direction, and pole class. Considering that the geographical area covered by the studied distribution network is relatively small, it is assumed that the wind speed and wind direction are the same throughout this area during a wind event. For simplicity, the peak demand of customers during summer is used to calculate EENS using Eq. (10). To accurately simulate the restoration process, a simulation time step of 0.5 h is used. It is assumed that the wind event occurs at the tenth hour of the simulation.

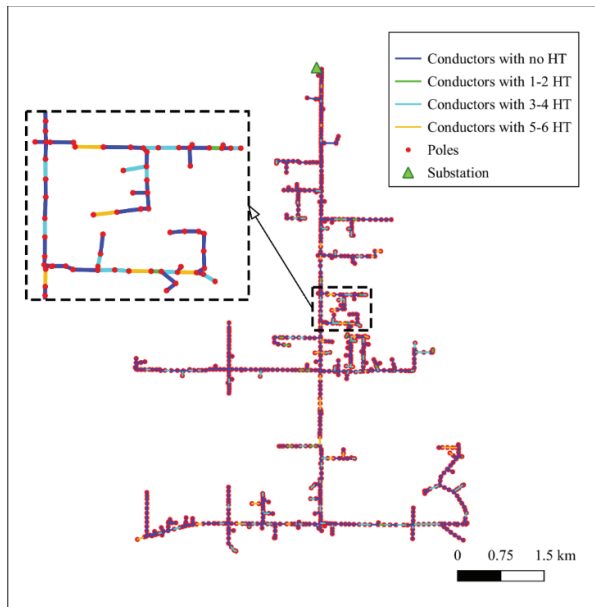


Fig. 5. A power distribution network in Oklahoma (Note: HT refers to hazard trees)

A. Windthrow fragility curves

Bur oak trees with heights ranging from 7 to 29 m are divided into 11 classes, and each class covers a height range of 2 m. Tree heights within each class follow uniform distributions. Windthrow fragility curves are developed for each height class. Statistics of wind load and mechanical properties of Bur oak trees used in the fragility analysis are given in Table 1. Fig. 6 shows the stem breakage and uprooting fragility curves of Bur oak trees with five height classes: 9-11 m, 13-15 m, 17-19 m, 21-23 m, and 25-27 m. It is observed that as the tree height increases, the stem breakage probability increases while the uprooting probability decreases. This can be explained by the low resistive moment at the root of smaller trees and the large wind loads and crown weight of big trees.

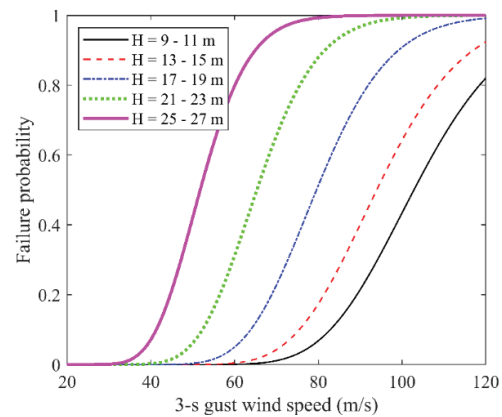
TABLE 1 STATISTICS OF MECHANICAL PROPERTIES OF BUR OAK TREES AND WIND LOAD PARAMETERS

Variables	Dist ^a	COV	CDF
Stem density (kg/m ³)	580	0.1	N ^b
Modulus of rupture (MPa)	49.6	0.16	N
Modulus of elasticity (MPa)	6070	0.22	N
Crown to stem weight ratio	0.3	0.25	N
Regression constant (NmKg ⁻¹)	67	0.2	N
Drag coefficient of crown	0.25	0.2	N
Drag coefficient of stem	1	0.1	N
Streamlining coefficient	0.4	0.2	N
Crown shape	Triangle		D ^c
Stem taper equation	-		D

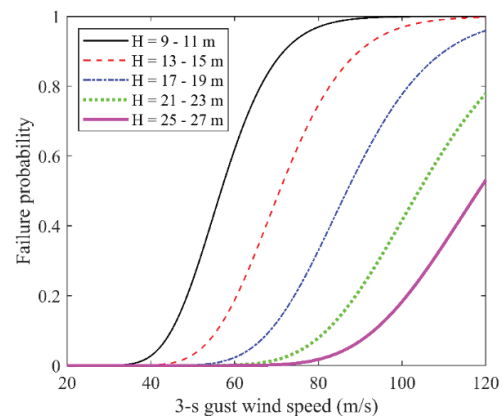
^a. Distribution

^b. Normal distribution

^c. Deterministic



(a) Breakage



(b) Uprooting

Fig. 6. Fragility curves of Bur oak trees

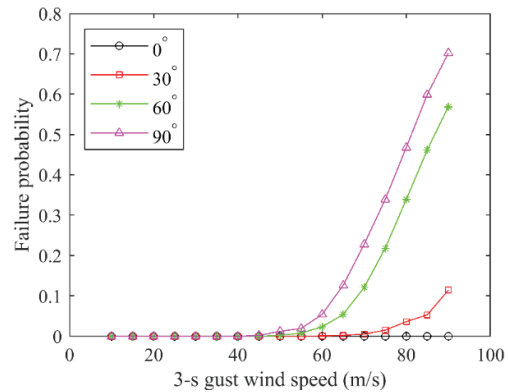
B. PDS component fragility curves

Fragility curves are developed for the 1-phase and 3-phase power systems with three pole classes (Class 2, 4, and 5) in the studied network. Table 2 provides the statistics of parameters used in PDS component fragility modeling. Fragility curves of the 3-phase power system with class 2 poles under wind loads are given in Fig. 7. Four wind attack angles are considered: 0°, 30°, 60°, and 90°. It can be seen in Fig. 7(a) that the most critical wind attack angle for pole failure is 90°. In this case, winds are perpendicular to the power lines and the pole failure probability is the highest. When the wind attack angle is 0°, pole failure doesn't occur when the wind speed is less than 90 m/s because there are no wind loads on the conductors. As shown in Fig. 7(b), similarly, the conductor breakage probability increases with the wind attack angle. However, as compared to the pole failure, the probability of conductor breakage is much lower.

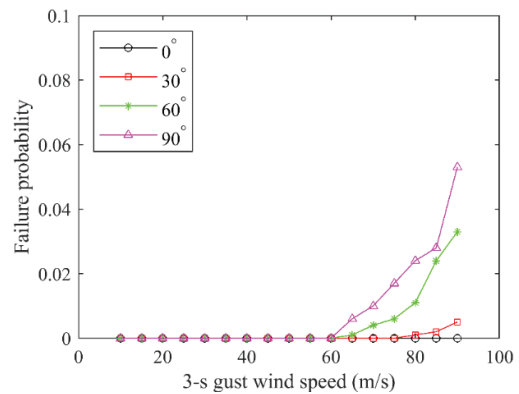
TABLE 2 STATISTICS OF PARAMETERS USED IN PDS COMPONENT FRAGILITY MODELING

Parameter	Dist ^a	Mean	COV
Span (m)	N ^b	63.72	0.433
Height of each pole class (m)	DP ^c	-	-
Fiber strength (MPa)	LN ^d	55.2	0.169
Wood density (kg/m ³)	N	500	0.04
Wood elastic modulus (GPa)	LN	14.68	0.04
Density of ACSR conductor (kg/m ³)	LN	3131.2	0.203
Diameter of ACSR conductor (mm)	LN	7.29	0.240
Breaking strength of ACSR conductor (MPa)	LN	406.5	0.247
Force coefficient	N	1	0.12
Gust effect factor of pole	N	0.97	0.11
Gust effect factor of wire	N	0.88	0.11
Exposure coefficient of pole	N	1	0.06
Exposure coefficient of wire	N	1.1	0.06
Pole diameter (mm)	D ^e	-	-
Elastic modulus of fiberglass crossarm (GPa)	D	75.84	-
Elastic modulus of ACSR conductor (GPa)	D	81	-
Density of fiberglass crossarm (kg/m ³)	D	2768	-

^a Distribution
^b Normal distribution
^c Discrete probability distribution
^d Lognormal distribution
^e Deterministic



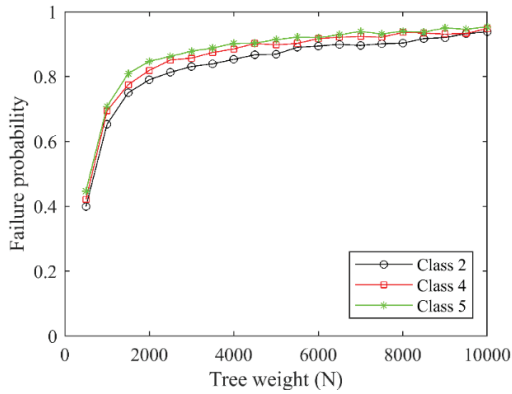
(a) Pole failure



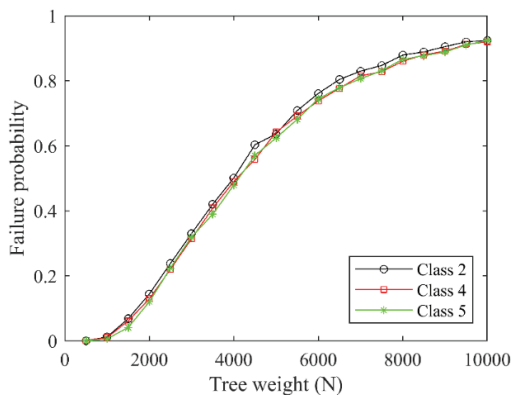
(b) Conductor breakage

Fig. 7. Fragility curves of 3-phase power system with class 2 poles under wind loads

Fragility curves of the 1-phase power system with different pole classes under tree loads are shown in Fig. 8. As shown in Fig. 8(a), the probability of short circuit can be high even under a relatively small tree load. The system with higher pole classes is more vulnerable to short circuit. Due to smaller diameter, poles with higher classes are easier to deform under the same tree load, further leading to larger deformation of conductors. In contrast, conductor breakage probability decreases as the pole class increases, as shown in Fig. 8(b). However, the difference is very small. It is also observed that short circuit is more prevalent than conductor breakage for a given tree load.



(a) Short circuit



(b) Conductor breakage

Fig. 8. Fragility curves of 1-phase power system with different pole classes under tree loads

C. Resilience assessment of PDS subjected to extreme winds

The resilience of the power distribution network for different wind scenarios is assessed in this subsection. Fig. 9 shows restoration curves for scenarios with different wind speeds but the same wind direction $\theta = 0^\circ$ (Northwind). As the wind speed increases, the network performance decreases, and the recovery time increases. It is also observed that the change is nonlinear, and the rate of change becomes larger with increasing wind speed.

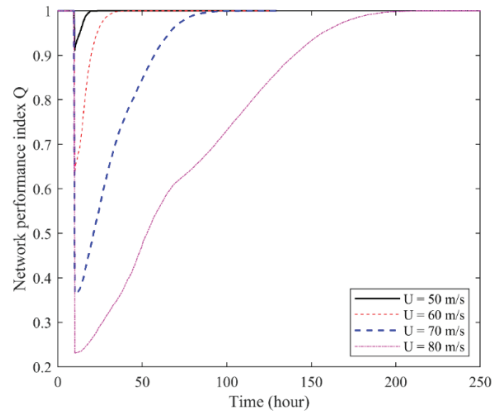


Fig. 9. Restoration curves for scenarios with different wind speeds ($\theta = 0^\circ$)

To understand the how the wind direction affects the power distribution network resilience, scenarios with different wind directions ($\theta = 0^\circ, 45^\circ, 90^\circ, 135^\circ, 180^\circ$) and the same wind speed ($U = 70 \text{ m/s}$) are studied. Fig. 10 gives restoration curves for scenarios with different wind directions. It is found that both the network performance and recovery time vary with the wind direction. By setting the control time as 120 hours, the resilience index RI values for the five scenarios are 0.85, 0.78, 0.76, 0.71, and 0.79. There is no obvious pattern between the resilience index and the wind direction. This can be explained by the network topology and the tree distribution.

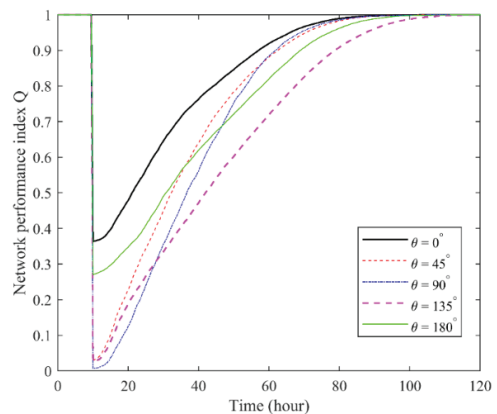


Fig. 10. Restoration curves for scenarios with different wind directions ($U = 70 \text{ m/s}$)

To understand the tree failures on the system resilience, scenarios with and without trees are studied and compared. Fig. 11 presents restoration curves for four scenarios under a wind speed of 70 m/s, namely, scenario 1, $\theta = 45^\circ$, with trees; scenario 2, $\theta = 45^\circ$, without trees; scenario 3, $\theta =$

225°, with trees; scenario 4, $\theta = 225^\circ$, without trees. It is found in Fig. 11 that the restoration curves of scenarios 2 and 4 overlap almost perfectly. This is because the network in the two scenarios suffers the same damage due to symmetry when tree failures are not considered. By comparing scenarios with and without trees, it is found that the network performance decreases, and the recovery time increases when tree failures are considered in scenarios 1 and 3. The resilience index RI reduces by 9% and 24% for scenarios 1 and 3 respectively, when the control time is set as 120 hours.

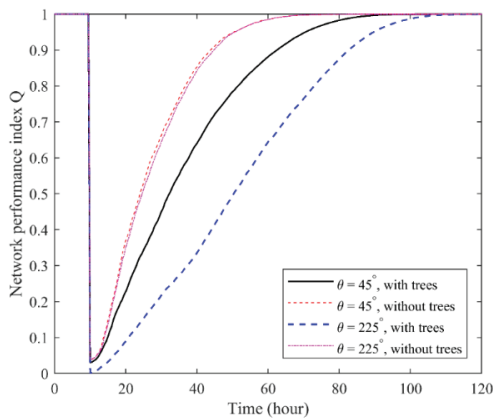


Fig. 11. Restoration curves for scenarios with and without considering trees ($U = 70$ m/s)

D. Resilience enhancement with vegetation management

Crown thinning is used to improve the PDS resilience against extreme winds. Normally, the live foliage that can be thinned from a tree must be less than 25% to avoid damaging its health. For the crown thinning method in this study, it is assumed that 25% of the crown is removed from all identified hazard trees in the network. It is also assumed that the crown density and effective crown area will be reduced by 25% and other tree parameters will remain the same after crown thinning. This will lead to a 25% reduction in both crown weight and wind loads acting on the crown. Fig. 12 shows the fragility curves of Bur oak trees with a height of 13-15 m before and after crown thinning. Both breakage and uprooting probability reduces after crown thinning. The reduction in EENS and restoration time with crown thinning are shown in Figs. 13 and 14, respectively. As shown in Figs. 13 and 14, crown thinning can effectively enhance the system resilience by reducing the EENS and restoration time. The reduction in EENS and restoration time increases with the wind speed and then decreases after reaching a peak at $U = 70$

m/s. This indicates that crown thinning will become less effective in enhancing the system resilience when the wind speed is very low or high.

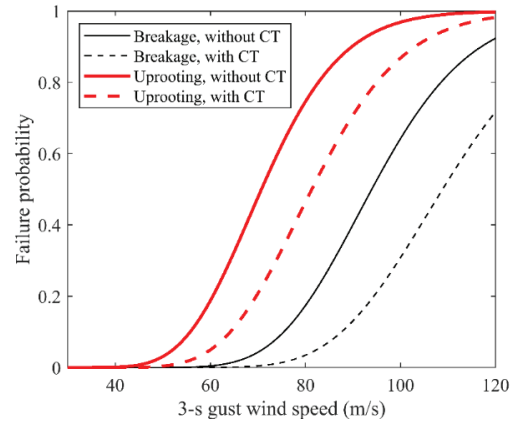


Fig. 12. Fragility curves of Bur oak before and after crown thinning

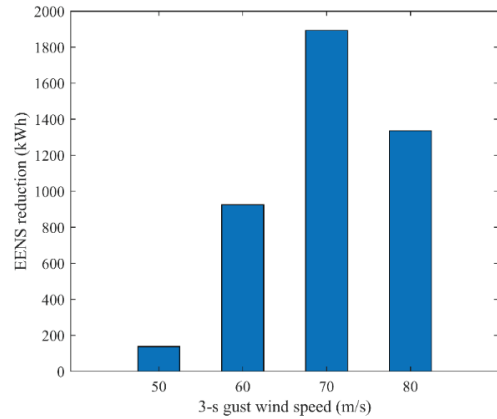


Fig. 13. Reduction in EENS with crown thinning

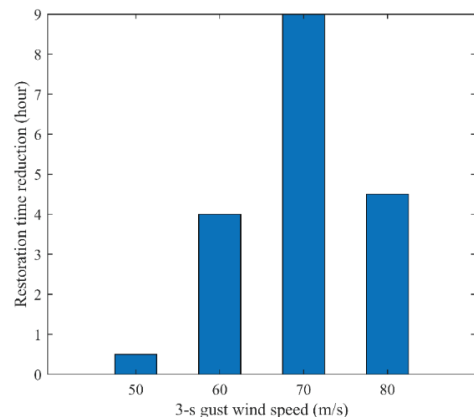


Fig. 14. Reduction in restoration time with crown thinning

IV. CONCLUSIONS AND FUTURE WORK

This paper proposes a probabilistic simulation framework for modeling the resilience of PDS to extreme winds, in which the impact of falling trees is considered. An example is presented to demonstrate the applicability of the framework. In the example, the resilience of a power distribution network in Oklahoma is assessed, and the vegetation management method for enhancing the system resilience is evaluated. Some conclusions have been drawn as follows:

- For Bur oak trees, with the increase of the tree height, the stem breakage probability increases while the uprooting probability decreases.
- Under wind loads, the failure probability of PDS components increases with the wind attack angle.
- Under tree loads, the short circuit is more prevalent than conductor breakage.
- The system resilience varies with the wind direction, but the variation depends on the topology of the network and the distribution of the trees.
- When tree failures are considered, the system resilience can reduce by 24%.
- Crown thinning can effectively enhance the system resilience by reducing the EENS and restoration time but will become less effective when the wind speed is very low or high.

This study can be improved with future work. For example, the failure of branches and limbs can be considered with a refined finite element tree model. In addition, the PDS component failure estimation model can be improved by considering the dynamic effect of falling trees.

ACKNOWLEDGMENT

This material is based on work supported by the U.S. National Science Foundation under Grant No. OIA-1946093. Any opinions, findings, and conclusions or recommendations expressed in this paper are those of the authors and do not necessarily reflect the views of the National Science Foundation.

REFERENCES

- [1] G. Li, P. Zhang, P. B. Luh, W. Li, Z. Bie, C. Serna, et al. "Risk Analysis for Distribution Systems in the Northeast U.S. Under Wind Storms," *Ieee T Power Syst.* 2014, vol. 29, pp. 889-898.
- [2] G. Y. Hou and S. R. Chen, "Probabilistic modeling of disrupted infrastructures due to fallen trees subjected to extreme winds in urban community," *Nat Hazards.* 2020, vol. 102, pp. 1323-1350.
- [3] G. Kakareko, S. Jung, E.E. Ozguven, "Estimation of tree failure consequences due to high winds using convolutional neural networks," *International Journal of Remote Sensing,* 2020, vol. 41, pp. 9039-9063.
- [4] Q. Lu, W. Zhang, "An integrated damage modeling and assessment framework for overhead power distribution systems considering tree-failure risks," *Struct Infrastruct E,* 2022.
- [5] G. Y. Hou, K. K. Muraleetharan, V. Panchaloganjan, P. Moses, A. Javid, H. Al-Dakheeli, et al. "Resilience assessment and enhancement evaluation of power distribution systems subjected to ice storms," unpublished.
- [6] M. Ouyang and L. Duenas-Osorio, "Multi-dimensional hurricane resilience assessment of electric power systems," *Struct Saf.* 2014, vol. 48, pp. 15-24.